2

Electrochemical Properties of Carbon-Supported Metal Nanoparticles Prepared by Electroplating Methods

Misoon Oh and Seok Kim
Pusan National University,
South Korea

1. Introduction

1.1 Pt and Pt-Ru catalysts for direct methanol fuel cells

There is a great demand for more potent, lightweight, efficient and reliable power-sources for a variety of transportation, portable electronics and other applications (Lamm et al., 2003). Batteries and fuel cells are alternative energy devices but batteries are only viewed as a short/mid-term option (Kuk & Wieckowski, 2005). Since transportation represents a significant portion of world energy consumption and contributes considerably to atmospheric pollution, the development of an appropriate **fuel cell** system is an important issue from both economical and environmental points of view (Arico et al., 2001). **Direct methanol fuel cells (DMFCs)** are an attractive portable power source owing to their high energy density, easy fuel handling, and a low operating temperature (Arico at al., 2000; Chen & Tang, 2002; Ren et al., 2000; Witham at al., 2003). However, DMFCs entail some serious technical obstacles. One is the relatively slow kinetics of the methanol oxidation reaction at an anode (Lima at al., 2001). Methanol oxidation reaction involves the transfer of six electrons to the electrode for complete oxidation to carbon dioxide. From a general point of view, almost all electro-oxidation reactions involving low molecular weight organic molecules, such as CO, CH_3OH, C_2H_5OH, HCOOH, HCHO, require the presence of **a Pt-based catalyst** (Arico at al., 2001). Platinum (Pt) has a high activity for methanol oxidation (Katsuaki at al., 1988, 1990; Watanabe at al., 1989). **Pt** is involved in two key steps occurring during the methanol oxidation route. One is the dehydrogenation step and the second is the chemisorption of CO (Arico at al., 2001). Pt electrocatalyst will be poisoned by intermediates of methanol oxidation, such as CO. To solve this problem, Pt was alloyed with other transition metals. Since the mid-1970s, to promote methanol electro-oxidation by Pt, the catalyst surface has been modified by the addition of a second metal to Pt (Gotz & Wedt, 1998; Hamnett at al., 1988; Mukerjee at al., 1999). The resulting Pt–Ru binary metallic catalyst is commonly accepted as the best electrocatalyst for methanol oxidation (Chu & Jiang, 2002; Gasteiger at al., 1993; Ticianelli at al., 1989; Ueda at al., 2006). In commercializing fuel cells, one of the most critical problems is the cost of metal catalysts deposited on electrodes (Chen at al., 2005; Frelink at al., 1995; Guo at al., 2005; Xiong & Manthiram, 2005; Kim at al., 2005; Kuk & Wieckowski, 2005; Qiao at al., 2005). Generally, platinum (Pt) or platinum alloy-based nanoclusters, which are impregnated on carbon supports, are the best

electrocatalysts for anodic and cathodic reaction of direct methanol fuel cells (DMFCs). These catalyst materials are very expensive, and thus there is a need to minimize the catalyst loading, without sacrificing electro-catalytic activity. One way to maximize catalyst utilization is to enhance the external Pt specific surface area per unit mass of Pt. The most efficient way to achieve this goal is to reduce the size of the Pt clusters. It is reported that the particle size and distribution of Pt-based catalysts are key factors that determine their electrochemical activity and cell performance for DMFCs (Kim at al., 2006; Kim & Park, 2006, 2007; Liang at al., 2003). The activity depends also on the morphological structure of the metal–carbon composite electrode (i.e. carbon surface area, carbon aggregation, metal dispersion, and metal–carbon interaction, etc.).

1.2 Supporting materials for metal catalysts

Supporting materials are also important factor to control the size of the metal catalysts particles and their dispersion. The ideal support material should have the following characteristics: provide a high electrical conductivity, have adequate water-handling capability at the cathode, and also show good corrosion resistance under oxidizing conditions. Different substrates for catalyst particles have been tried, with the aim of improving the efficiency of methanol electro-oxidation. Generally, the electrocatalysts are supported on high-surface-area **carbon blacks** with a high mesoporous distribution and graphite character, and XC-72 carbon black is the most widely used carbon support because of its good compromise between electronic conductivity and the BET surface area. However, this conventional carbon supported catalyst offers only a low rate of methanol oxidation, partly due to low utilization of Pt, owing in turn to a low available electrochemical specific surface area for the deposition of Pt particles (Shi, 1996). Moreover, Vulcan XC-72 carbon particles generally contain sulfur groups, causing some side reaction and possibly resulting in Pt particle aggregation (Roy at al., 1996). Accordingly, considerable effort has been devoted to the development of new carbon support materials to improve both the oxidation rate and the electrode stability in methanol oxidation. Carbon supports include graphite nanofibers (GNFs), carbon nanotubes (CNTs), carbon nanocoils (CNCs), and ordered microporous carbons (OMCs) (Joo at al., 2001; Li at al., 2003; Rajesh at al., 2000; Steigerwalt at al., 2001). Novel modified carbon species have been studied as the support materials for catalyst deposition in order to obtain an available surface area, better catalyst dispersion, and the resulting high electroactivity.

Conducting polymers can be also used as suitable host matrices for dispersing metallic particles. Conducting polymer/metal-nanoparticles composites permit a facile flow of electronic charges through the polymer matrix during the electrochemical process. Additionally, electrical conducting polymers provide a low ohmic drop of electron transfer between the metal catalyst and the substrates. Also, metallic particles can be dispersed into the matrix of these polymers. By combining conducting polymers and metal particles, it is expected that novel electrodes with higher specific surface areas and enhanced electrocatalytic activities could be prepared. Recently, Y. E. Sung et al. proposed that Pt–Ru nanoparticles/electrical conducting polymer nanocomposites are effective as anode catalysts (J. H. Choi at al., 2003). At that time, the electrical conductivity of polymers was relatively low compared with amorphous carbon, and synthetic methods were limited to electrochemical polymerization from nonaqueous systems. In previous studies (Kost at al.,

1988; Lai at al., 1999), metal particles could be homogeneously dispersed on polyaniline film by constant potential electro-plating techniques. However, in our study, step-potential electroplating methods were utilized to obtain a smaller size and a better electrochemical activity.

1.3 Electrodepositon

Pulse electrodeposition has many advantages in terms of controlled particle size, stronger adhesion, uniform electrodeposition, selectivity of hydrogen, reduction of internal stress, etc. Pulse electrodeposition has three independent variables, namely, t_{on} (on-time), t_{off} (off-time) and i_p (peak current density). The properties of metal deposits can be influenced by both the on-time, during which formation of nuclei and growth of existing crystals occur, and the off-time, during which desorption of deposited ions takes place.

Electrochemical deposition occurs at cathode electrode and the deposited metal ions are exhausted along the electrodeposition. Eventually, the ion concentration at the cathode surface becomes zero. The current density at which dendrite crystals begin to form is defined as the 'limiting current density'. At this current density, the ion concentration at the deposited surface is zero. Pulse electrodeposition can raise the limiting current density because the deposited metal ions of the cathode surface can be supplied from the bulk solution during the off-time of the pulse (K. H. Choi at al., 1998).

Recently, electrochemical deposition of metal catalysts has been receiving more and more attention due to advantages such as the high purity of deposits, the simple deposition process, and the easy control of the loading mass. By applying a short-duration specific current or potential, and then repeating the process during electrodeposition, each cycle of this process can generate new metal particles (Laborde at al., 1994). Therefore, by controlling the magnitude of the current/potential and applied time, nanoparticles can be altered in size and structure. The size and dispersion of catalyst particles on the substrate determine the catalysts' performance as an electrode material.

Lee and co-workers proposed that Pt nanoparticles as catalysts for proton exchange membrane fuel cells be prepared by pulse electrodeposition (K. H. Choi at al., 1998). As they reported, a current pulse electrodeposition method resulted in better catalytic activity than did direct current (dc) electrodeposition, owing to the larger effective surface area of catalyst. In previous studies (Coutanceau at al., 2004; Kost at al., 1988; Lai at al., 1999), metal particles have successfully been homogeneously dispersed on support by constant potential electro-plating techniques.

The aim of this study was not only to overcome the problem of the complexity of catalyst preparation by using a simple electrodeposition, but also to control the size and loading level of metal particles. Furthermore, an optimal electrical signal condition, such as a certain step interval or plating time, was sought in order to enable the manufacture of a catalyst electrode offering improved catalytic activity. Besides, the effect of carbon-like species including carbon nanotubes, graphite nanofibers and conducting polymers on the electrochemical activity of metal-carbon composite electrodes will be investigated. By performing the current-voltage characterization or electrochemical methods, the possibility of fuel-cell catalyst utilization will be presented. The morphology and micro-structure of carbon-supported metal particles will be also studied and the relationship with the catalyst activity is analyzed.

2. Preparation of Pt and Pt-Ru catalysts by electrochemical deposition

2.1 Deposition of Pt on graphite nanofiber by electrochemical potential sweep method

Carbon materials used were graphite nanofibers (GNFs), which were supplied by Showa Denko Co. (Japan). These carbon fiber materials have a diameter of 100~150nm and a length of 5~50μm, resulting a large aspect ratio.

Electrochemical deposition was performed using an Autolab with a PGSTAT 30 electrochemical analysis instrument (Eco Chemie B.V.; Netherlands). The carbon materials were coated on to glassy carbon substrate with the help of 0.1% Nafion solution. A 10mM hexachloroplatinic acid (H_2PtCl_6) was dissolved in 0.5M HCl aqueous solution. A potential was swept from -700mV to -200mV (vs. Ag/AgCl) with a sweep rate of 20mV/s. A large reduction peak is shown at about –600mV (vs. Ag/AgCl). The deposited catalyst electrodes are prepared with changing the sweep times.

2.2 Deposition of Pt-Ru on carbon nanotubes by step-potential plating method

Electrodeposition of Pt-Ru nanoparticles on support was performed using an Autolab with a PGSTAT 30 electrochemical analysis instrument (Eco Chemie B.V.; Netherlands). The solid precursors, chloroplatinic acid (H_2PtCl_4, Aldrich) and ruthenium chloride ($RuCl_3$, Aldrich), were used without purification. A standard three-electrode cell was employed. Carbon nanotubes (CNTs) were selected as the support material. The CNTs, supplied from Iljin Nanotech, Korea (Multiwalled nanotubes, Purity: >99 wt.%), were used without further purification. The CNTs were synthesized by a chemical vapor deposition (CVD) process.

The CNTs mixed with 10% Nafion® perfluorosulfonated ion-exchange resin (Aldrich) solution, were dropped onto a glassy carbon electrode, selected as the working electrode. A Pt wire as the counter electrode and KCl-saturated Ag/AgCl as the reference electrode were used, respectively. Pt-Ru nanoparticles were, by the step-potential plating method, electrodeposited on the CNTs catalyst electrodes in a distilled water solution containing ruthenium chloride and chloroplatinic acid. In the deposition solution, the atomic concentration of Pt and Ru was 20 mM, respectively. A potential function generator was used to control both the step-interval time and the plating time. The potential wave form of the deposition is shown in Figure 1. The catalysts were cycled in the range of -0.3 V to -0.8 V with interval times (t_1 and t_2) of 0.03, 0.06, 0.20, and 0.50 seconds. The plating time was 20 min in all cases. However, the catalysts were prepared by changing the plating time from 6 to 12, 24, and 36 min, using constant interval times (t_1 and t_2).

2.3 Deposition of Pt-Ru on conducting polymer supports and carbon supports by step-potential plating method

2.3.1 Support materials

CBs and polyaniline were used as a support for the metal catalysts. The CBs of 24 nm average particle size, and having a DBP adsorption of 153 (cc-100g^{-1}) and a specific surface area of 112 (m^2 g^{-1}), were supplied by Korea Carbon Black Co.

Polyaniline powder was synthesized chemically by oxidative polymerization of aniline in an aqueous acidic solution (Aleshin at al., 1999; Kim & Chung, 1998; MacDiarmid & Epstein,

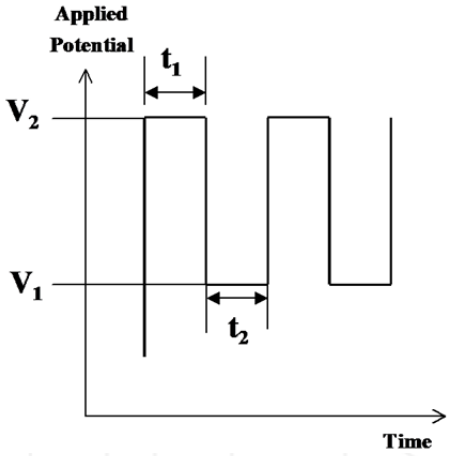

Fig. 1. Step-potential plating method showing parameters of applied potential and interval time.

1989). The aniline (8.4g, 0.09mol; Aldrich), distilled three times before use, was dissolved in 300 mL of aqueous solution containing 0.09 mol dodecylbenzene sulfonic acid (DBSA) below 5°C, and an aqueous solution (100 mL) of 0.06 mol ammonium peroxydisulfate, $(NH_4)_2S_2O_8$, was added with vigorous stirring, over a period of 30 min. The mixture was stirred continuously for 24 h. The precipitate was collected after pouring methanol and by filtration, and then washed with water and methanol three times. The resulting powder was dried under a dynamic vacuum at 40°C for 2 days. The DBSA-doped polyaniline was confirmed by measuring the electrical conductivity (~80 S/cm). The conductivity of CBs was 0.7 S/cm. PANI and CBs pellets, fabricated by compressing PANI and CBs powder under the pressure of 5.0×10^7 kg/m^2 at room temperature, were measured for conductivity using the four-probe method.

2.3.2 Electrodeposition of Pt-Ru nanoparticles on support

Electrodeposition of Pt-Ru nanoparticles on support was investigated using an Autolab with a PGSTAT 30 electrochemical analysis instrument (Eco Chemie B.V.; Netherlands). The solid precursors chloroplatinic acid (H_2PtCl_4, Aldrich) and ruthenium chloride ($RuCl_3$, Aldrich) were used without purification. A standard three-electrode cell was employed. The support materials mixed with 10% Nafion Perfluorosulfonated ion-exchange resin (Aldrich) solution was dropped onto the glassy carbon electrode as a working electrode. A Pt wire as the counter electrode and KCl-saturated Ag/AgCl as the reference electrode were used, respectively. Pt-Ru nanoparticles were, by step potential plating method, electrodeposited on the CB and polyaniline catalyst electrodes from distilled water solution containing ruthenium chloride and chloroplatinic acid. In the deposition solution, the concentration of Pt and Ru was 20 mM. A potential function generator was used to control both the step potential value and the interval time. The potential wave form of the deposition is shown in Figure 1. The catalysts were cycled in the range of -0.3 V to -0.8 V (V_1 and V_2) with an interval time (t_1 and t_2) of 0.1 seconds. The electrocatalysts were prepared by changing the plating time.

3. Characterization of Pt and Pt-Ru catalysts

3.1 Deposition of Pt on graphite nanofiber by electrochemical potential sweep method

3.1.1 Morphologies and structural properties

After Pt incorporation into carbon materials, the average crystalline sizes of Pt nanoparticles were analyzed by XRD measurements. Figure 2 shows the powder X-ray diffraction patterns of Pt catalysts deposited on GNFs as a function of sweep times. With an increase of sweep times, a sharp peak of Pt(111) at 2θ = 39° and a small peak at 2θ = 46° and 2θ = 67° increase gradually. This gradual changes of the peak intensity can be clearly explained by the fact that and Pt was deposited successively as new particles on GNFs surface and the loading level increase with the increase of sweep times. On the other hand, it can be shown that GNFs in this study have a crystalline graphitic structure due to the strong peak at 2θ = 26° and 2θ = 54°. All samples show the typical Pt crystalline peaks of Pt(111), Pt(200) and Pt(220).

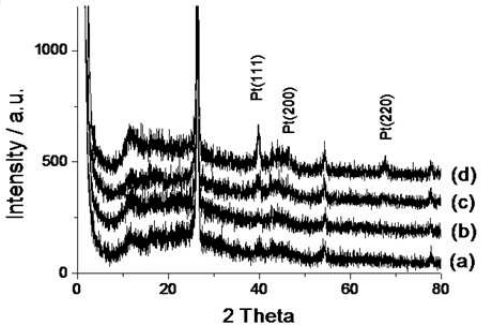

Fig. 2. Powder X-ray diffraction patterns of Pt/GNFs prepared by potential sweep method as a function of sweep times of (a) 6, (b) 12, (c) 18, and (d) 24 times.

The average size of Pt nanoparticles was calculated by using a Scherrer equation and was demonstrated in Table 1. The average size of Pt increased from 2.13nm to 8.94nm gradually by changing the sweep times of electrochemical deposition. It is interesting to note that a sharpness of peak is enhanced with an increase of sweep times.

Sample	Average size (nm)	Loading level (%)
Pt6	2.13	4
Pt12	2.90	7
Pt18	3.73	9
Pt24	8.94	11

Table 1. Average particle sizes and loading content of carbon-supported platinum catalysts as a function of sweep times.

The larger the sharpness of peaks is, the larger the average crystalline size of Pt particles is. The increase of Pt average size could be related to an aggregation of Pt nanoparticle by increasing the sweep times. It is expected that the deposited Pt particles are more

aggregated and become larger. From this result, it is concluded that the particle size can be changed by controlling the condition of electrochemical deposition methods.

3.1.2 Electrochemical properties

Platinum content can be calculated by ICP-AES method. The result is summarized in Table 1. In the viewpoint of Pt content, Pt24 shows the highest value of 11%, which means the loading level increased gradually with the sweep times. Figure 3 shows the electroactivity of Pt catalyst supported on the carbon supports by linear sweep voltammograms. Peak potentials and current density were shown in Table 2. Anodic peaks for a methanol oxidation were shown at 850 ~ 900 mV for each sample. The current density of anodic peaks increased from 0.08 mA cm-2 to 0.17 mA cm-2 by increasing sweep times from 6 to 18. However, a further increase of sweep times over 18 has brought a decrease of current density. The specific current densities for each sample were also shown in Table 2. The mass activity showed the maximum value of 204 mA/mg at 18 sweep times. This value is a similar level of value (~200 mA/mg) with the previous reports.

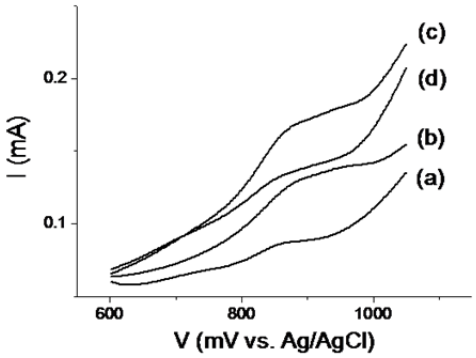

Fig. 3. I-V characteristic curves of Pt catalysts prepared by potential sweep method as a function of sweep times of (a) 6, (b) 12, (c) 18, and (d) 24 times (in 0.5M H_2SO_4 + 0.5M CH_3OH).

Sample	Peak Potential (mV)	Peak Current (μA)	Specific Activity (mA/mg)
Pt6	856	85	145
Pt12	870	125	186
Pt18	872	166	204
Pt24	860	131	120

Table 2. Peak parameters and specific activities for CV results of Pt/GNFs prepared by potential sweep method as a function of sweep times.

This means that the electrocatalytic activity has been decayed when the sweep times is over 18. Consequently, the electrocatalytic activity increased with sweep times upto 18 due to an increase of loading level of Pt. However, the electroactivity are decayed at excessive sweep times due to a large size of Pt nanocluster due to the aggregation.

Figure 4 shows impedance plots of catalysts in 0.5M H_2SO_4 + 0.5M CH_3OH. These plots were obtained by changing the frequency from 1 MHz to 0.1 Hz. The plots show an imperfect semi-circle part and a linear line part. The bulk resistance could be obtained by considering the real part of impedance at x-axis intercept. The bulk resistances were described in Figure 5. With an increase in sweep times from 6 to 18, the resistance decreased from 68 to 4 Ohm cm^2. With an increase in sweep times from 18 to 24, the resistance increased from 4 to 9 Ohm cm^2. The resistance change with sweep times showed a similar trend with the above electroactivity results. Considering together these results, the resistance change could be one of the origins for the electroactivity changes. It is thought that the resistance could be largely decreased by the improved electrical conduction between Pt particles and GNFs supports due to the enhanced loading levels.

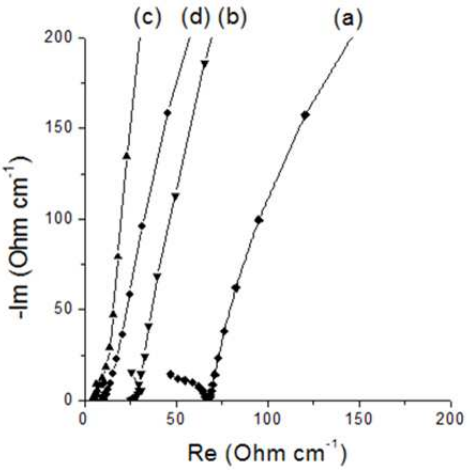

Fig. 4. Impedance plots of Pt catalysts prepared by potential sweep method as a function of sweep times of (a) 6, (b) 12, (c) 18, and (d) 24 times.

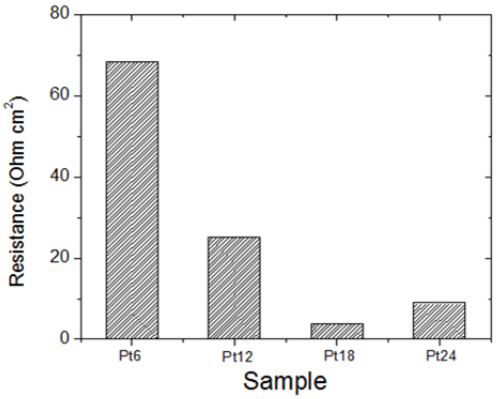

Fig. 5. Bulk resistance of Pt catalysts prepared by potential sweep method as a function of sweep times.

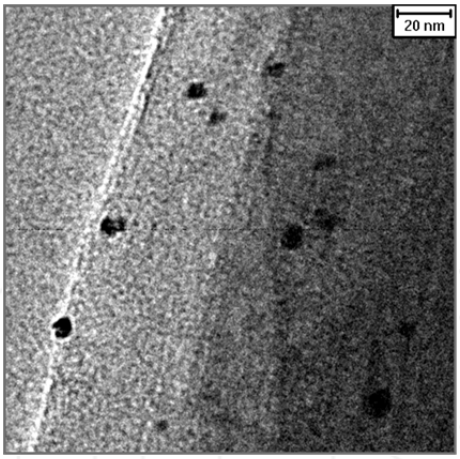

Fig. 6. TEM image of the Pt catalysts prepared by potential sweep method at 18 sweep times.

Figure 6 shows the TEM image of Pt nanoparticles deposited on GNFs supports prepared by electrochemical deposition. It has been clearly shown that 3-7nm nano-sized nanoparticles are successfully deposited and well-dispersed on GNFs surfaces. The appearance and population of particle are rather scarce due to the low loading level of 9 wt.%.

3.2 Pt-Ru on carbon nanotubes by step potential plating method

3.2.1 Size and loading level of catalysts

The crystalline structures of the Pt-Ru/CNTs catalysts were investigated by X-ray diffraction (XRD). Figure 7 shows the XRD patterns of the catalysts prepared by changing the step interval of the step-potential plating method. The peaks at 2θ = 40°, 47°, 68°, and 82° were associated with the (111), (200), (220), and (311) types of Pt, respectively. All of the catalysts demonstrated diffraction patterns similar to those of the Pt. In the case of the 0.03 sec interval, the catalyst showed a distinct characteristic peak and the strongest intensity. By

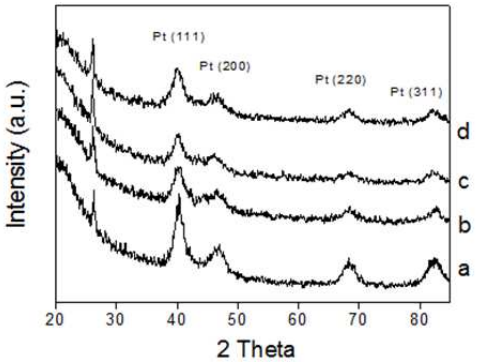

Fig. 7. X-ray diffraction patterns of PtRu/CNTs catalysts prepared by changing step interval from (a) 0.03 to (b) 0.06, (c) 0.20, and (d) 0.50 sec.

increasing the interval from 0.03 sec to 0.20 sec, the intensities of the four peaks were gradually changed. The loading contents of the catalysts were obtained separately by using ICP-AES methods, and are given in Table 3. The loading content of Pt degraded from 12.9% to 9.2%, and that of Ru changed from 7.8% to 4.7%. The weight and atomic ratio of PtRu were also described in Table 3.

Step interval (sec)	Loading of Pt (wt.%)	Loading of Ru (wt.%)	Weight ratio	Atomic ratio
0.03	12.9	7.8	1:0.61	1:1.17
0.06	11.5	6.4	1:0.56	1:1.07
0.2	10.4	5.5	1:0.53	1:1.02
0.5	9.2	4.7	1:0.51	1:0.99

Table 3. Loading level of PtRu/CNTs catalysts measured by ICP-AES method

Figure 8 shows the XRD patterns of the catalysts prepared by changing the plating time of the step-potential plating method. In the case of the 6 min plating time, the intensity of the characteristic peaks of Pt was rather small. After 24 min plating, the catalysts showed definite and enhanced peak intensities for the four kinds of peaks. The precise loading contents and PtRu ratio using the ICP-AES methods are given in Table 4. The loading content of Pt was upgraded from 4.7% to 13.1%, and that of Ru was changed from 2.4% to 8.2%.

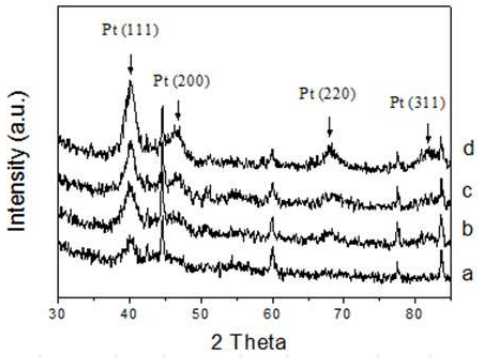

Fig. 8. X-ray diffraction patterns of PtRu/CNTs catalysts prepared by changing plating time from (a) 6 to (b) 12, (c) 24, and (d) 36 min.

Plating time (min)	Loading of Pt (wt.%)	Loading of Ru (wt.%)	Weight ratio	Atomic Ratio
6	4.7	2.4	1:0.51	1:0.98
12	8.2	4.5	1:0.55	1:1.06
24	10.4	6.1	1:0.59	1:1.13
36	13.1	8.2	1:0.63	1:1.21

Table 4. Loading level of PtRu/CNTs catalysts measured by ICP-AES method.

The average sizes of the CNTs-supported catalysts as a function of step interval and plating time are shown in Table 5 and Table 6, respectively. The average crystalline sizes were obtained by XRD measurements. The mean sizes of the particles were determined from the X-ray diffractograms, using the Scherrer equation (1) (Kinoshita, 1988)

$$L = \frac{0.9\lambda}{B_{2\theta}\cos\theta_{\max}} \quad (1)$$

where λ is the X-ray wavelength (1.54056 Å for the CuKα radiation), $B_{2\theta}$ is the width of the diffraction peak at half-height, and θ_{max} is the angle at the peak maximum position.

Step interval (sec)	Crystalline size from XRD (nm)	Particle size from TEM (nm)
0.03	6.2 ± 0.2	6.4 ± 0.3
0.06	4.6 ± 0.1	4.8 ± 0.3
0.2	6.4 ± 0.2	6.8 ± 0.4
0.5	8.2 ± 0.3	9.1 ± 0.5

Table 5. Mean particle size of PtRu/CNTs catalysts obtained by XRD and TEM methods.

Plating time (min)	Crystalline size from XRD (nm)	Particle size from TEM (nm)
6	7.4 ± 0.2	7.9 ± 0.5
12	6.3 ± 0.2	6.7 ± 0.4
24	4.1 ± 0.1	4.3 ± 0.2
36	11.2 ± 0.4	11.5 ± 0.5

Table 6. Mean particle size of PtRu/CNTs catalysts obtained by XRD and TEM methods.

Particle sizes were also listed by TEM methods. In the case of the changed step intervals, the smallest particle size was obtained with the 0.06 sec interval. By increasing the interval time to 0.50 sec, the particle size was gradually increased, reflecting the growth of the deposited particles. It was concluded that the 0.06 sec interval is the best condition for obtaining the smallest particle size. Therefore, the 0.06 sec interval was used to study the effect of changed plating time on the catalytic activity.

The average catalyst nanoparticle size was 7.9 nm at 6 min plating time. It was considered that particle nucleation is not as efficient as particle growth at the initial stage of electrodeposition. After 24 min plating, the particle nucleation was efficient enough to produce a new generation of small particles, resulting in the decrease of the average particle size. Although more precise nucleation and growth mechanisms are necessary for Pt-Ru nanoparticles, it was found that the smaller particle size could be obtained after an initial activation state. The smallest nanoparticles of 4.3 nm were obtained by electrodeposition after 24 min plating time. It was concluded that this is the optimal plating time for obtaining the smallest particle catalysts.

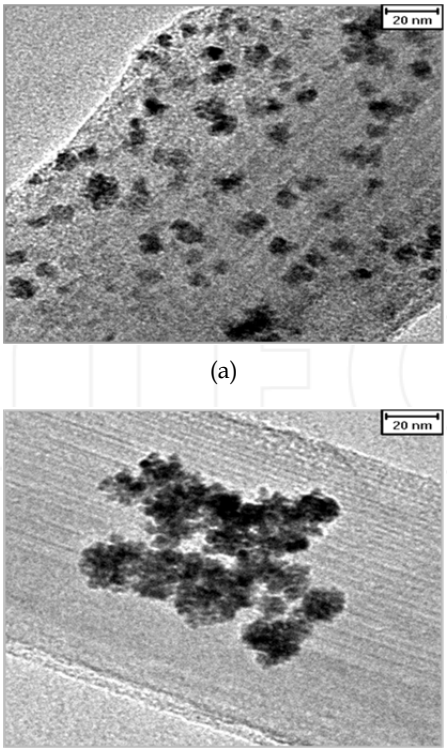

(a)

(b)

Fig. 9. TEM micrograph of PtRu/CNTs catalysts prepared by (a) 0.03 sec and (b) 0.5 sec step intervals.

The particle sizes and morphologies of the CNTs-supported Pt-Ru catalysts were investigated by TEM. Figure 9 shows TEM images of nanoparticle catalysts that were prepared on CNTs by electrodeposition at 0.06 sec and 0.50 sec interval times, which showed the smallest and the largest particle size, respectively. In the case of (a) the 0.06 sec interval, the image shows well-dispersed 3-6 nm nanoparticles on the surface of the CNTs. In contrast to this, in the case of (b) the 0.50 sec interval, the image shows rather aggregated catalyst particles of 5 – 8 nm size. It could be concluded that with increased the step-interval time, particles tend to increase in size, and also, to an extent, to aggregate. The TEM images of catalysts prepared by different plating times and a constant 0.06 sec step interval, are also shown in Figure 10. In the case of (a) the 6 min plating time, the population of the deposited particles, arranged in nanoclusters with individual particle sizes ranging from 5 to 7 nm, is rather low, reflecting the low loading content at the early state of deposition. In the case of (b) the 24 min plating time, the population of the particles, ranging in size from 3 to 5 nm, was enhanced, manifesting the increased loading content. The average particle size, as can be seen, was decreased in the case of the 24 min plating time. And the average crystalline sizes calculated from the XRD peak widths were found to be fairly consistent with particle sizes from the TEM results, as shown in Table 5 and Table 6.

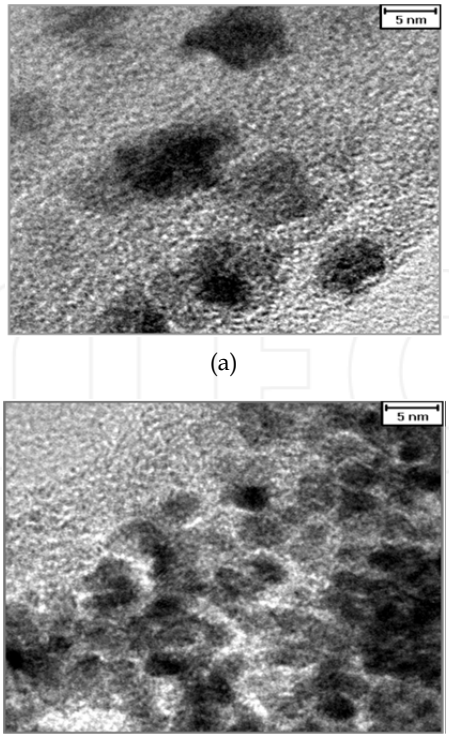

Fig. 10. TEM micrograph of PtRu/CNTs catalysts prepared with (a) 6 min and (b) 24 min plating times.

3.2.2 Electrochemical properties of catalysts

The electrochemical properties of the catalysts were investigated by linear sweep voltammetry in 1 M CH_3OH + 0.5 M H_2SO_4 aqueous solution. Figure 11 shows the current-voltage curves of the CNTs-supported catalysts, representing the electrochemical behavior of methanol oxidation. The electrochemical activities of catalysts prepared by changed step intervals were studied. In the case of the 0.03 sec interval, the catalyst curve shows a slight oxidation peak at 780 mV and an increasing current density. In the case of the 0.06 sec interval, the curve shows a slight oxidation peak at 740 mV and, again, an increasing current density. The oxidation peak was shifted to the low potential, indicating the more feasible oxidation reaction of methanol. Furthermore, the current density was higher than in the case of the 0.03 sec interval. In the cases of 0.20 sec and 0.50 sec intervals, in contrast, the oxidation peak was not clearly shown, and the current density of the catalyst was degraded. These results indicate that the electro-plating step intervals over 0.20 sec can have a negative influence on the electrochemical activity of deposited catalysts.

Figure 12 shows the current-voltage curves of the CNTs-supported catalysts prepared by changed step intervals. At the early stage of 6 and 12 min plating, the current density at the same potential was increased gradually with the plating time, meaning that the catalytic

activity was increased by the enhanced loading contents. In the case of 24 min plating, the curve shows a slight oxidation peak at 730 mV, a different phenomenon from those for the other samples. Furthermore, an onset potential, which is the potential of oxidation current to begin to rise, was shifted to the lower potential of ~500 mV. The onset potentials for the other samples, were ~800 mV. It was concluded, accordingly, that the electrochemical activity was highly improved in this case of 24 min plating, which advance was related to the fact that smaller particles and higher dispersion of catalysts result in a larger available catalyst surface area and better electrocatalytic properties for methanol oxidation.

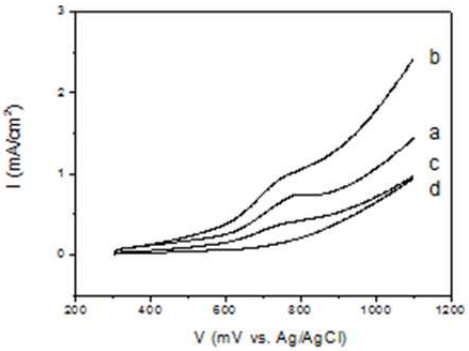

Fig. 11. Current-voltage curves of PtRu/CNTs catalysts prepared by changing step interval from (a) 0.03 to (b) 0.06, (c) 0.20, and (d) 0.50 sec.

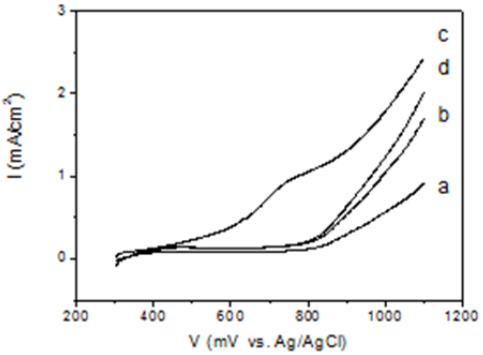

Fig. 12. Current-voltage curves of PtRu/CNTs catalysts prepared by changing plating time from (a) 6 to (b) 12, (c) 24, and (d) 36 min.

The electrochemical activity increased with increasing plating time, reaching the maximum at 24 min, and then decreased at 36 min. However, the catalysts showed an increased Pt content, in proportion to the plating time, to 36 min. That is, the Pt content was the highest when the plating time was 36 min, even though the optimal plating time, as we saw, was 24min. This puzzling result was considered to have originated in the catalyst's smallest, 4.3 nm particle size and highest specific surface area. These electroactivity changes as a function of electrical condition were inversely proportional to the size of the nanoparticle catalysts, strongly indicating that the higher electroactivity could have been enabled by the decreasing

average size of nanoparticle catalysts, resulting in the increase of the efficient specific surface area for an electro-catalytic reaction.

Figure 13 shows the weight-based current densities of the prepared catalysts, according to the above conditions. At the 0.06 sec step-interval, as shown by graph (A), the specific current densities of the catalysts showed the highest value, 160 (mA/mg). At step intervals over 0.06 sec, the current density was degraded, increasingly with each interval. When the plating time was increased to 24 min, the specific current density of catalysts, as shown by graph (B), was gradually enhanced to 202 (mA/mg). However, the 36 min plating time showed a decreased value of deposited catalyst. Therefore, it could be deduced that the electroactivity of catalysts prepared by electrodeposition is strong dependent on the electrical signal condition manifest in the step interval and the plating time.

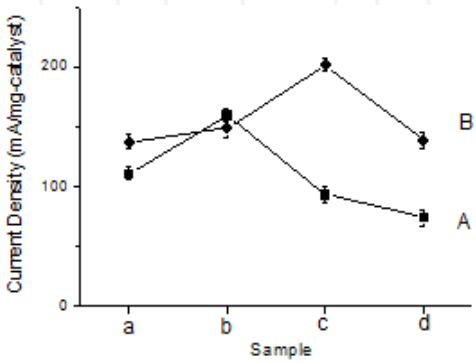

Fig. 13. Specific current density of PtRu/CNTs catalysts prepared (A) by changing step interval from (a) 0.03 to (b) 0.06, (c) 0.20, and (d) 0.50 sec, or (B) by changing plating time from (a) 6 to (b) 12, (c) 24, and (d) 36 min.

To check the specific surface area of catalysts, cyclic voltammograms (CVs) had been perfored. Figure 14 shows the CVs of the prepared catalysts in 1.0M sulphuric acid solution and the calculated electrochemical surface area are listed in Table 7. Catalyst by 0.06 sec interval time showed the highest specific surface area. In the case of changing the plating time, the specific surface area was increased upto 24 min plating time and then was decreased. Over 24 min plating, the particle was thought to be overlapped causing the decrease of the specific surface area and slight increase in particle size. This result supported that the catalytic activity was strongly dependent on the particle size and specific surface area.

3.3 Pt-Ru on conducting polymer supports and carbon supports by step potential plating method

3.3.1 Size and loading level of catalysts

The crystalline structures of the Pt-Ru/CBs and Pt-Ru/polyaniline catalysts were investigated by X-ray diffraction (XRD). Figure 15 and Figure 16 show the XRD patterns of the catalysts prepared by changing the plating time of the step-potential plating method. The peaks at $2\theta = 40°$, 47°, 68°, and 82° were associated with the (111), (200), (220), and (311)

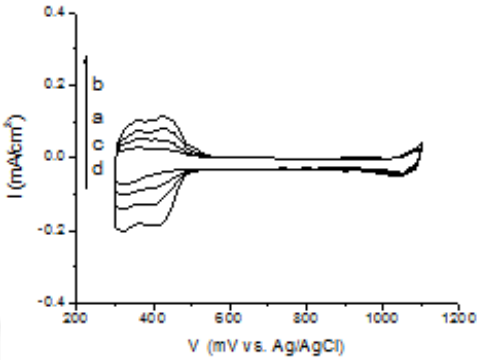

(a)

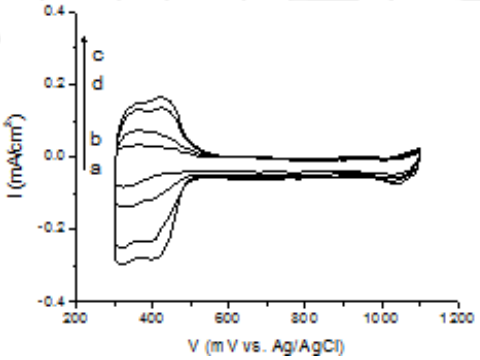

(b)

Fig. 14. Cyclic voltammograms of PtRu/CNTs catalysts prepared (A) by changing step interval from (a) 0.03 to (b) 0.06, (c) 0.20, and (d) 0.50 sec and (B) by changing plating time from (a) 6 to (b) 12, (c) 24, and (d) 36 min.

(a)	Step interval (sec)	Electrochemical surface area (cm^2)	Specific surface (m^2/g)
	0.3	3.21	63.2
	0.6	4.26	89.5
	0.2	2.16	51.7
	0.5	1.21	43.3
(b)	Plating time (sec)	Elctrochemical surface area (cm^2)	Specific surface area (m^2/g)
	6	1.97	71.8
	12	3.53	83.2
	24	6.83	98.2
	36	6.14	68.2

Table 7. Surface area of catalyst by changing (a) step interval and (b) plating time that was calculated from the H_2 absorption peak in CVs (Figure 14).

types respectively. All of the catalysts demonstrated diffraction patterns similar to those of the Pt. The characteristic peaks for Ru were not clearly shown in the XRD patterns. In the case of the 6 min plating time, the characteristic peaks of Pt were not distinct, indicating inefficient electrodeposition of the metal catalysts. For the 12 min plating time, Pt(111) appeared at ~40°. After 24 min plating, the catalysts showed definite and enhanced peak intensity for the four kinds of peaks. In the case of 36 min plating, the catalysts clearly showed the characteristic peaks. The precise loading contents of the catalysts were obtained by using ICP-AES methods, and are given in Table 8. The loading content of Pt was upgraded from 2.1% to 7.2%, and that of Ru was changed from 1.0% to 3.1%. The loading content had been increased proportionally as a function of plating time.

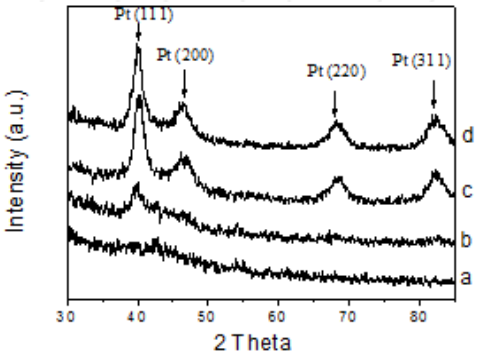

Fig. 15. X-ray diffraction patterns of Pt-Ru/CBs catalysts prepared for different plating times of (a) 6, (b) 12, (c) 24, and (d) 36 min.

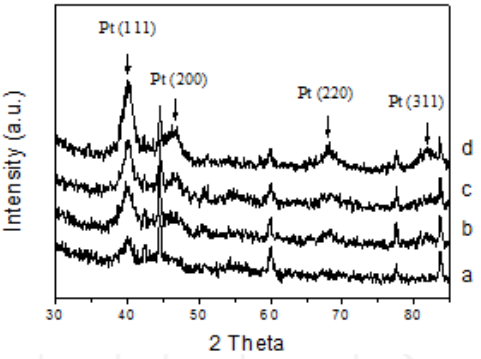

Fig. 16. X-ray diffraction patterns of Pt-Ru/polyaniline catalysts prepared for different plating times of (a) 6, (b) 12, (c) 24, and (d) 36 min.

Similar to the Figure 15 results, and as shown in Figure 16, the crystalline peaks of the polyaniline-supported catalysts were not clearly evident for the initial plating time of 6 min, except for the appearance of a small Pt (111) peak. After 12 min plating, the catalysts showed the four characteristic peaks. With increasing plating time after 24 min, the peaks became sharp and definite.

Plating time (min)	Crystalline size (nm)[a]	Particle size (nm)[b]	Pt (wt.%)[c]	Ru (wt.%)[c]	Alloyed Ru (%)
6	-	8.1	2.1	1.0	21
12	5.2± 0.3	5.4	3.9	1.2	24
24	3.4± 0.2	3.6	6.1	2.1	32
36	4.2± 0.2	4.6	7.2	3.1	26

Table 8. Mean size and loading contents of Pt-Ru/CBs catalysts.; a: measured from XRD results, b: measured from TEM results, c: measured from ICP-AES results.

Plating time (min)	Crystalline size (nm)[a]	Particle size (nm)[b]	Pt (wt.%)[c]	Ru (wt.%)[c]	Alloyed Ru (%)
6	-	7.4	2.3	1.3	20
12	4.3± 0.3	4.5	7.6	3.1	25
24	2.9± 0.2	3.1	9.3	4.6	35
36	3.9± 0.3	4.2	11.1	5.3	27

Table 9. Mean size and loading contents of Pt-Ru/polyaniline catalysts.; a: measured from XRD results, b: measured from TEM results, c: measured from ICP-AES results.

Considering particle crystalline size, the average sizes of CBs-supported catalysts showed the smallest value, 3.4 nm, at 24 min plating, as shown in Table 1. Beside, particle sizes by TEM results were shown in Table 8 and Table 9. In the case of 6 min plating time, the average size was ~8 nm. It was considered that particle nucleation was not as efficient as the particle growth at the initial stage of electrodeposition. After 24 min plating, the particle nucleation was efficient enough to produce a new generation of small particles, resulting in the decrease of the average crystalline size. Although more precise nucleation and growth mechanisms are necessary for Pt-Ru nanoparticles, it was found that the smaller crystalline size could be obtained after an initial activation state. This behavior was also observed in the case of polyaniline supports, as shown in Table 9. Regardless of the support materials, the smallest nanoparticles were obtained by electrodeposition after 24 min plating time. The loading content of Pt or Ru was 11.1% or 5.3%, respectively, after 36 min plating time. These values were slightly higher that those of the CBs supports. It was concluded that conducting polymer supports are more beneficial for a higher loading for electrodeposition of catalysts.

The peak position of PtRu catalysts had been shifted in comparison with that of pure Pt catalyst. The shift of peak position could mean the change of a lattice parameter.

We had calculated the alloying degree by the following formula (Antoline & Cardellini, 2001);

$$l_{PtRu} = 0.3916 - 0.124 x_{Ru} \tag{2}$$

(where l_{PtRu} is the lattice parameter of PtRu catalysts, and x_{Ru} is the percent of Ru in the alloy) The lattic parameter of PtRu is smaller than that of Pt, meaning a part of Ru had entered into the crystal lattice of Pt. The alloying degree of Ru had been inserted in Table 8 and 9.

The particle sizes and morphologies of the Pt-Ru/CBs and Pt-Ru/polyaniline catalysts were investigated by TEM. Figure 17 shows a TEM image of nanoparticle catalysts that were prepared on CBs by electrodeposition with plating time. 24 min plating showed the smallest particle sizes. This shows the nanoparticles in the 2.5-5.0 nm size range. Figure 18 shows a TEM image of catalysts that were prepared on polyaniline supports with changing plating time. 24 min plating shows nanoclusters with individual particles of 2.5-4.1 nm size. The average crystalline sizes calculated from the XRD peak widths were found to be fairly consistent with those from the TEM results, as shown in Table 8 and Table 9.

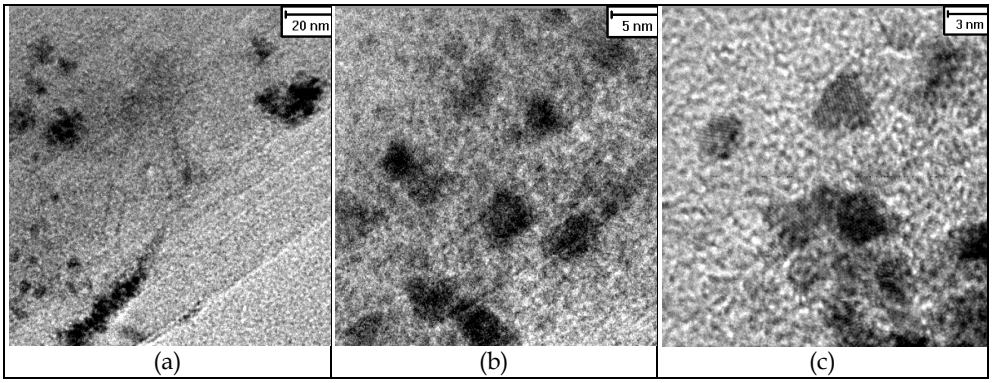

Fig. 17. TEM micrograph of Pt-Ru/CBs catalysts by (a) 6 min, (b) 12 min, and (c) 24 min plating time.

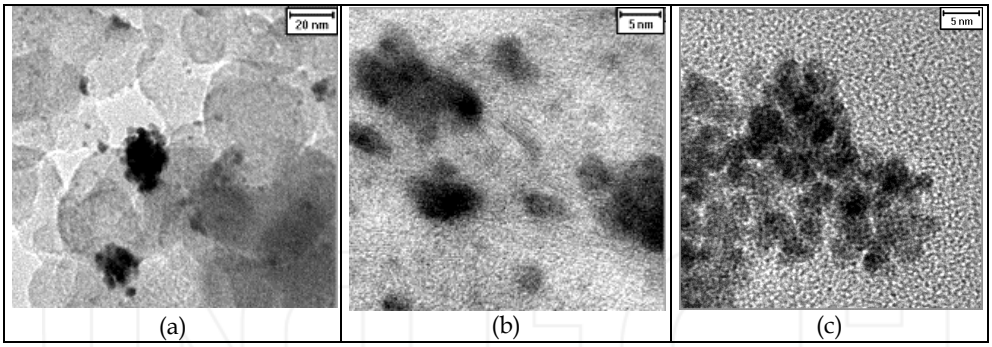

Fig. 18. TEM micrograph of Pt-Ru/polyaniline catalysts by (a) 6 min, (b) 12 min, and (c) 24 min plating time.

3.3.2 Electrochemical properties of catalysts

The electrochemical properties of the catalysts were investigated by cyclic voltammetry in 1 M CH_3OH + 0.5 M H_2SO_4 aqueous solution. Figure 19 shows the representative current-voltage curves of the CBs-supported catalysts, presenting the electrochemical behavior of methanol oxidation. Voltammetric behavior depends on the Pt content. The electrochemical activity increased with increasing plating time, reaching the maximum at 24 min, and then slightly decreased. However, the catalysts showed an increased Pt content with plating time

to 36 min. The optimal plating time was 24min, although the Pt content was the highest when the plating time was 36 min. The catalyst by 24 min plating showed the highest current density for methanol oxidation, indicating the highest electroactivity by an enhanced specific surface area of a reaction site for metallic catalysts. This result was considered to have been originated from the catalyst's smaller particle size and lower aggregation.

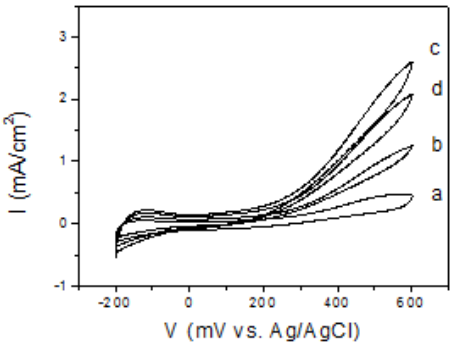

Fig. 19. Cyclic voltammograms of Pt-Ru/CBs catalysts prepared for different plating times of (a) 6, (b) 12, (c) 24, and (d) 36 min in 1 M methanol solution (scan rate: 20mV/s).

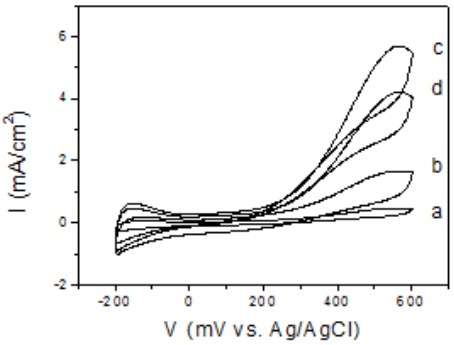

Fig. 20. Cyclic voltammograms of Pt-Ru/polyaniline catalysts prepared for different plating times of (a) 6, (b) 12, (c) 24, and (d) 36 min in 1 M methanol solution (scan rate: 20mV/s).

In the case of the polyaniline-supported catalysts, the cyclic voltammograms shown in Figure 20 also exhibit methanol oxidation peak. The catalyst deposited on PANI showed a rather definite oxidation peak at ~520 mV. Similar to the CBs supports, the catalysts showed the highest electroactivity at 24 min plating. Indeed, the catalysts by 24 min plating exhibited an average size of 3.1 nm, whereas the catalysts by 36 min plating showed an average size of 4.2 nm. Smaller particles of catalysts might result in a large available catalyst surface area and good electrocatalytic properties for methanol oxidation.

To determine the carbon and PANI support influences, individually, on the oxidation current of catalysts, supports without metal catalysts were studied in 1 M CH_3OH + 0.5 M H_2SO_4 aqueous solution, as shown in Figure 21. The carbon support did not show any electrochemical activity except for some small capacitive current. By contrast, the PANI support showed a

definite cathodic/anodic peak, indicating an oxidation/reduction reaction (Aleshin at al., 1999; Kim & Chung, 1998; MacDiarmid & Epstein, 1989). However, it was concluded that polyaniline supports could not function alone as catalysts for methanol oxidation.

To check the specific surface area of catalysts, cyclic voltammograms (CVs) had been performed. Figure 22 shows the CVs of the PANI- or CBs-supported catalysts in 1.0M sulphuric acid solution. H_2 adsorption/desorption peak were observed at –200 mV for both case and the electrochemical surface area are calculated (PtRu/PANI: 4.3 cm^2, PtRu/CBs: 7.4 cm^2). By considering the different metal loading, we obtained the specific surface area by dividing the metal weight (PtRu/PANI: 62 m^2/g, PtRu/CBs: 75 m^2/g). Catalyst deposited on PANI showed the higher specific surface area than PtRu/CBs. This result supported that the effective surface area could be dependent on the particle size and aggregation degree.

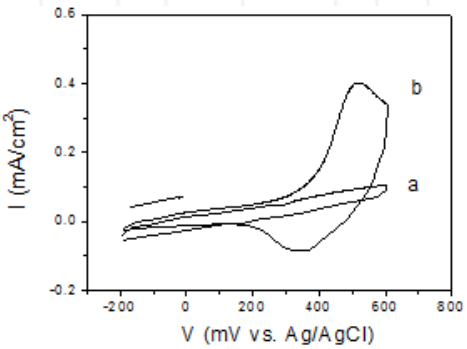

Fig. 21. Cyclic voltammograms of (a) CBs and (b) polyaniline supports in 1 M methanol solution (scan rate: 20mV/s).

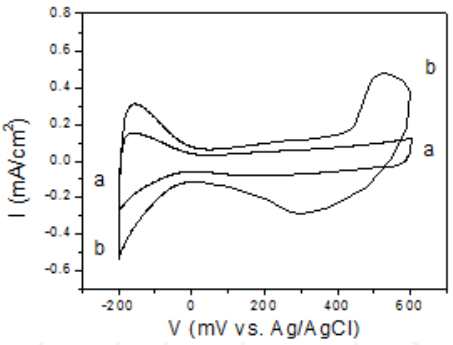

Fig. 22. Cyclic voltammograms of (a) Pt-Ru/CBs and (b) Pt-Ru/polyaniline prepared by 24 min plating in 1 M sulfuric acid solution (scan rate: 20mV/s).

Beside, chronoamperometry could be used to obtain the apparent diffusion coefficient of ions in electrochemical reactions. The current responses with time were shown in Figure 23. After the potential was raised abruptly from -0.2 to 0.6V, the current response was recorded. Using a following equation, the apparent diffusion coefficient had been calculated (Antoline & Cardellini, 2001; Bard & Faulkner, 1980).

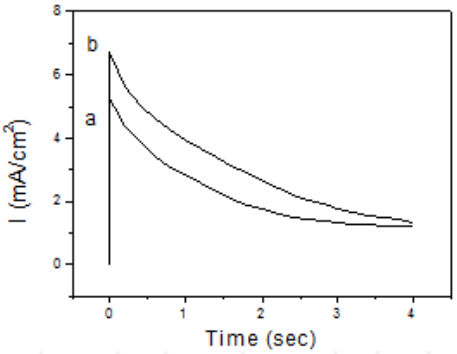

Fig. 23. Chronoamperometry results of (a) Pt-Ru/CBs and (b) Pt-Ru/polyaniline by 24 min plating in 1 M methanol solution.

$$\ln\left(\frac{i}{i_O}\right) = -\frac{\pi^2 D}{l^2} t \tag{3}$$

where i_o is the initial current, i the current, l sample thickness and t the time.

The obtained diffusion coefficients were like following; PtRu/PANI: 6.1×10^{-9} cm/s, PtRu/CBs: 4.2×10^{-9} cm/s. The former case was a higher value than the latter case. This result could be one of the reasons of the improved electroactivity.

Figure 24 shows the specific current densities of the prepared Pt-Ru/CBs and Pt-Ru/polyaniline catalysts. The current densities of the different materials-supported catalysts as a function of plating time showed similar behaviours. The PANI-supported catalysts showed enhanced electroactivity compared with the carbon-supported catalysts. In the early stage of 6 min plating, the difference of enhanced current density (41-9 = 32 (mA/mg)) was almost similar to the current density (27 (mA/mg)) of PANI itself. However, in the case of 24 min plating, the difference of increased current density (121-68 = 53 (mA/mg)) was much higher

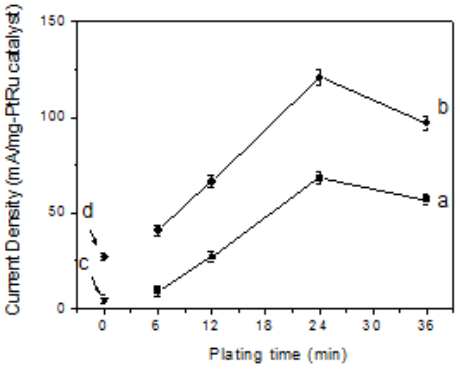

Fig. 24. Specific current density for oxidation peaks of (a) Pt-Ru/CBs and (b) Pt-Ru/polyaniline catalysts prepared for different plating times ((c) CBs and (d) polyaniline supports themselves were added for comparison) (at 600 mV).

than the current density of PANI itself. Accordingly, it was concluded that the improved electroactivity of the PANI-supported catalysts was a result not only of the combined activity of the catalysts and the PANI; one of the main sources of the improved electroactivity was the high electronic conductivity of DBSA-doped polyaniline (~80 S/cm) compared with that of the CBs (~0.7 S/cm) (Aleshin at al., 1999). Additionally, we had found that the electrochemical area of catalysts had been increased. The increased electrochemical area might be related to the small particle size and low degree of aggregation.

4. Conclusions

The electrochemical deposition and characterization of Pt and Pt-Ru nanoparticles on carbons and conducting polymer supports were investigated. Pt and Pt-Ru particles were successfully electrodeposited by electrochemical potential sweep and step-potential plating methods.

At the electrochemical potential sweep method, the average size and loading level of Pt particles increased gradually with increase of potential sweep times. The electroactivity of Pt catalyst electrode showed a highest performance at 18 sweep times due to the best particle size and loading level. It was thought that excessive sweep time brought the decay of electroactivity due to the larger particle size and degraded particle dispersion. It was concluded that the smallest particle size and the smallest bulk resistance could influence the improved activity.

The particle size and loading level of Pt-Ru was also controlled by step-potential plating method. It was found that a smaller interval time under same plating time enabled a higher loading content of electro-deposited metal particles. By contrast, Pt loading content was enhanced with the increase of plating time. With increased step interval time, particles tended to increase in size, and also, to an extent, to aggregate. These results correlated to the fact that smaller particles and higher available catalyst surface area could bring the better electrocatalytic properties for methanol oxidation. The specific surface area was confirmed by measuring the H_2 absorption peak. This result supported that the catalytic activity was strongly dependent on specific surface area.

Finally, the properties of the Pt-Ru catalysts were affected by support materials. Pt-Ru/CBs showed 68mA/mg, Pt-Ru/polyaniline showed 121mA/mg, and Pt-Ru/CNTs showed 202mA/mg for values of methanol oxidation specific current. The electroplating method and the physic-chemical feature of support materials affected the deposited particle size of Pt-Ru catalysts and tendency of aggregation.

5. Acknowledgment

This research was supported by the Converging Research Center Program through the Ministry of Education, Science and Technology (Grant No.: 2011K000643), the Ministry of Knowledge and Economy (Material source Technology Project Grant No. 10037238.2011), and Basic Science Research Program through the National Research Foundation of Korea (NRF) funded by the Ministry of Education, Science and Technology (Grant No.: 2011-0009007).

6. References

Aleshin, A.N.; Lee, K.; Lee, J.Y.; Kim, D.Y. & Kim, C.Y. Comparison of electronic transport properties of soluble polypyrrole and soluble polyaniline doped with dodecylbenzene-sulfonic acid. *Synth. Met.*, Vol.99, No.1, (January 1999), pp. 27-33.

Antoline, E. & Cardellini, F. Formation of carbon supported PtRu alloys: an XRD analysis. *J. Alloys Compd.*, Vol.315, No.1-2, (February 2001), pp. 118-122.

Arico, A.S.; Creti, P.; Modica, E.; Monforte, G.; Baglio, V. & Antonucci, V. Investigation of direct methanol fuel cells based on unsupported Pt–Ru anode catalysts with different chemical properties. *Electrochim. Acta*, Vol.45, No.25-26, (August 2000), pp. 4319-4328.

Arico, A.S.; Srinivasan, S. & Antonucci, V. DMFCs: from fundamental aspects to technology development. *Fuel Cells*, Vol.1, No.1 (September 2001), p. 133-161.

Bard, A.J. & Faulkner, L.R. Electrochemical Method, *Wiley*, New York, 1980 Chapter. 3,6, and 10.

Chen, C.Y. & Tang, P. Performance of an air-breathing direct methanol fuel cell. *J. Power Sources*, Vol.123, No.1, (September 2003), pp. 37-42.

Chen, C.Y.; Yang, P.; Lee, Y.S. & Lin, K.F. Fabrication of electrocatalyst layers for direct methanol fuel cells. *J. Power Sources*. Vol.141, No.1, (February 2005), pp. 24-29.

Choi, J.H.; Park, K.Y.; Kim, Y.M.; Lee, J.S. & Sung, Y.E. Nano-composite of PtRu alloy electrocatalyst and electronically conducting polymer for use as the anode in a direct methanol fuel cell. *Electrochim. Acta*. Vol.48, No.9, (August 2003), pp. 2781-2789.

Choi, K.H.; Kim, H.S. & Lee, T.H. Electrode fabrication for proton exchange membrane fuel cells by pulse electrodeposition. *J. Power Sources*. Vol.75m No.2, (October 1998), pp. 230-235.

Chu, D. & Jiang, R. Novel electrocatalysts for direct methanol fuel cells. *Solid State Ionics*, Vol.148, No.3-4, (June 2002), pp. 591-599.

Coutanceau, C.; Rakotondrainibe, A.; Lima, A.; Garnier, E.; Pronier, S.; Leger, J.M. & Lamy, C. Preparation of Pt-Ru bimetallic anodes by galvanostatic pulse electrodeposition: Characterization and application to the direct methanol fuel cell. *J. Appl. Electrochem.*, Vol.34, No.1, (January 2004), pp. 61-65.

Frelink,T.; Visscher, W. & Rvan, J.A. Particle size effect of carbon-supported platinum catalysts for the electrooxidation of methanol. *J. Electroanal. Chem.*, Vol. 382, No.1-2, (February 1995), pp. 65-72.

Gasteiger, H.A.; Markovic, N.; Ross, P.N. & Cairns, E.J. Methanol electrooxidation on well-characterized Pt-Ru alloys. *J. Phys. Chem.*, Vol.97, No.46, (1993), pp. 12020-12029.

Gotz, M. & Wendt, H. Binary and ternary anode catalyst formulations including the elements W, Sn and Mo for PEMFCs operated on methanol or reformate gas. *Electrochim. Acta*, Vol.43, No.24, (August 1998), pp. 3637-3644.

Guo, J.W.; Zhao, T.S.; Prabhuram, J. & Wong, C.W. Preparation and the physical/electrochemical properties of a Pt/C nanocatalyst stabilized by citric acid for polymer electrolyte fuel cells. *Electrochim. Acta*. Vol.50, No.10, (March 2005), pp. 1973-1983.

Hamnett, A.; Kenndey, B.J. & Weeks, S.A. Base metal oxides as promotors for the electrochemical oxidation of methanol. *J. Electroanal. Chem.*, Vol.240, No.1-2, (January 1988), pp. 349-353.

Joo, S.H.; Choi, S.J.; Oh, I.; Kwak, J.; Liu, Z.; Terasaki, O. & Ryoo, R. Ordered nanoporous arrays of carbon supporting high dispersions of platinum nanoparticles. *Nature*. Vol.412, No.6843, (July 2001), pp. 169-172.

Katsuaki, S.; Kohei, U.; Hideaki, K. & Yoshinobu, N. Structure of Pt microparticles dispersed electrochemically onto glassy carbon electrodes: Examination with the scanning tunneling microscope and the scanning electron microscope. *J. Electroanal. Chem.*, Vol.256, No.9, (December 1988), pp. 481-487.

Katsuaki, S.; Ryuhei, I. & Hideaki, K. Enhancement of the catalytic activity of Pt microparticles dispersed in Nafion-coated electrodes for the oxidation of methanol by RF-plasma treatment. *J. Electroanal. Chem.*, Vol.284, No.2, (May 1990), pp. 523-529.

Kim, S. & Chung, I.J. Annealing effect on the electrochemical property of polyaniline complexed with various acids. *Synth. Met.*, Vol.97, No.2, (September 1998), pp. 127-133.

Kim, S.; Cho, M.H.; Lee, J.R.; Ryu, H.J. & Park, S.J. Electrochemical Behaviors of Platinum Catalysts Deposited on the Plasma Treated Carbon Blacks Supports. Kor. Chem. Eng. Res. Vol.43, (2005), pp. 756-760.

Kim, S.; Cho, M.H.; Lee, J.R. & Park, S.J. Influence of plasma treatment of carbon blacks on electrochemical activity of Pt/carbon blacks catalysts for DMFCs. *J. Power Sources*. Vol.159, No.1, (September 2006), pp. 46-48.

Kim, S. & Park, S.J. Effects of chemical treatment of carbon supports on electrochemical behaviors for platinum catalysts of fuel cells. *J. Power Sources.* Vol.159, No.1, (September 2006), pp. 42-45.

Kim, S. & Park, S.J. Effect of acid/base treatment to carbon blacks on preparation of carbon-supported platinum nanoclusters. *Electrochim. Acta*. Vol.52, No.9, (February 2007), pp. 3013-3021.

Kinoshita, K. Carbon: Electrochemical and Physicochemical Properties, *John Wiley*, New York, 1988, p. 31.

Kost, K.M.; Bartak, D.E.; Kazee, B. & Kuwana, T. Electrodeposition of platinum microparticles into polyaniline films with electrocatalytic applications. *Anal. Chem.*, Vol.60, No.21, (1988), pp. 2379-2384.

Kuk, S.T. & Wieckowski, A. Methanol electrooxidation on platinum spontaneously deposited on unsupported and carbon-supported ruthenium nanoparticles. *J. Power Sources,* Vol.141, No.1, (February 2005), pp. 1-7.

Laborde, H.; Leger, J.M.; & Lamy, C. Electrocatalytic oxidation of methanol and C1 molecules on highly dispersed electrodes Part II: Platinum-ruthenium in polyaniline. *J. Appl. Electrochem.*, Vol.24, No.10, (October 1994), pp. 1019-1027.

Lai, E.K.W.; Beattie, P.D.; Orfino, F.P.; Simon, E. & Holdcroft, S. Electrochemical oxygen reduction at composite films of Nafion®, polyaniline and Pt. *Electrochim. Acta*. Vol.44, No.15, (1999), pp. 2559-2569.

Lamm, A.; Gasteiger, H.; Vielstich, W. (Eds.), (2003). *Handbook of Fuel Cells*, Wiley-VCH, Chester, UK.

Li, W.; Liang, C.; Qiu, J.; Zhou, W.; Qiu, J.; Zhou, Z.; Sun, G. & Xin, Q. Preparation and Characterization of Multiwalled Carbon Nanotube-Supported Platinum for Cathode Catalysts of Direct Methanol Fuel Cells. *J. Phys.Chem. B*. Vol.107, No.26, (2003), pp. 6292-6299.

Lima, A.; Cutanceau, C.; Leger, J.M. & Lamy, C. Investigation of ternary catalysts for methanol electrooxidation. *J. Appl. Electrochem.*, Vol.31, No.4, (April 2001), pp. 379-386.

MacDiarmid, A.G. & Epstein, A.J. Polyanilines: A novel class of conducting polymers. *Faraday Discuss. Chem. Soc.*, Vol.85, (1989), pp. 317-332.

Mukerjee, S.; Lee, S.J.; Ticianelli, E.A.; Mcbreen, J.; Grgur, B.N.; Markovic, N.M.; Ross, R.N.; Giallombardo, J.R. & Castro, De E.S. Investigation of enhanced CO tolerance in proton exchange membrane fuel cells by carbon supported PtMo alloy catalyst. *Electrochem. Solid-State Lett.*, Vol.2, No.1, (1999), pp. 12-15.

Qiao, H.; Kunimatsu, M. & Okada, T. Pt catalyst configuration by a new plating process for a micro tubular DMFC cathode. *J. Power Sources*. Vol.139, No.1-2, (January 2005), pp. 30-34.

Rajesh, B.; Ravindranathan, T.K.; Bonard, J.M. & Viswanathan, B. Preparation of a Pt–Ru bimetallic systemsupported on carbon nanotubes. *J. Mater. Chem.*, Vol.10, (June 2000), pp. 1757-1759.

Ren, X.; Zelenay, P.; Thomas, S.; Davey, J. & Gottesfeld, S. Recent advances in direct methanol fuel cells at Los Alamos National Laboratory. *J. Power Sources*, Vol.86, No.1-2, (March 2000), pp. 111-116.

Roy, S.C.; Christensen, P.A.; Hamnett, A.; Thomas, K.M. & Trapp, V. Direct Methanol Fuel Cell Cathodes with Sulfur and Nitrogen-Based Carbon Functionality. *J. Electrochem. Soc.*, Vol.143, No.10, (October 1996), pp. 3073-3079.

Shi, H. Activated carbons and double layer capacitance. *Electrochim. Acta.* Vol.41, No.10, (June 1996), pp. 1633-1639.

Steigerwalt, E.S.; Deluga, G.A.; Cliffel, D.E. & Lukehart, C.M. A Pt-Ru/graphitic carbon nanofiber nanocomposite exhibiting high relative performance as a direct-methanol fuel cell anode catalyst. *J. Phys. Chem. B*, Vol.105, No.34, (August 2001), pp. 8097-8101.

Ticianelli, E.; Beery, J.G.; Paffett, M.T. & Gottesfeld, S. An electrochemical, ellipsometric, and surface science investigation of the PtRu bulk alloy surface. *J. Electroanal. Chem.*, Vol.258, No.1, (January 1989), pp. 61-77.

Ueda, S.; Eguchi, M.; Uno, K.; Tsutsumi, Y. & Ogawa, N. Electrochemical characteristics of direct dimethyl ether fuel cells. *Solid State Ionics.* Vol.177, No.19-25, (October 2006), pp. 2175-2178.

Watanabe, M.; Saeguae, S. & Stonelhart, P. High platinum electrocatalyst utilizations for direct methanol oxidation. J. Electroanal.Chem., Vol.271, No.1-2, (June 1989), pp. 213-220.

Witham, C.K.; Chun, W.; Valdez, T.I. & Narayanan, S.R. Performance of direct methanol fuel cells with sputter-deposited anode catalyst layers. *Electrochem. Solid-State Lett.* Vol.3, No.11, (November 2000), pp. 497-500.

Xiong, L. & Manthiram, A. Catalytic activity of Pt–Ru alloys synthesized by a microemulsion method in direct methanol fuel cells. *Solid State Ionics*. Vol.176 , No.3-4, (January 2005), pp. 385-392.

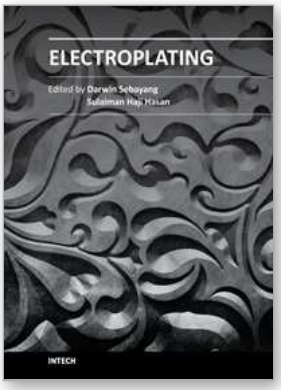

Electroplating

Edited by Prof. Darwin Sebayang

ISBN 978-953-51-0471-1
Hard cover, 166 pages
Publisher InTech
Published online 11, April, 2012
Published in print edition April, 2012

This book emphasizes on new applications of electroplating with consideration for environmental aspect and experimental design. Written by experienced expert from various countries, the authors come from academia and electroplating industrial players. Here, a very detailed explanation to the new application of the electroplating is followed by a solution of the environmental issue caused by the electroplating process and concluded by experimental design for optimization of electro deposition processes.

Coverage included:
- Preparation NiO catalyst on FeCrAl Subtrate Using Various Technique at Higher Oxidation Process
- Electrochemical properties of carbon- supported metal nanoparticle prepared by electroplating methods
- Fabrication of InGaN-Based Vertical Light Emitting Diodes Using Electroplating
- Integration Of Electrografted Layers for the Metallization of Deep Through Silicon Vias
- Biomass adsorbent for removal of toxic metal ions from electroplating industry wastewater
- Resistant fungal biodiversity of electroplating effluent and their metal tolerance index
- Experimental design and response surface analysis as available tools for statistical modeling and optimization of electrodeposition processes

How to reference

In order to correctly reference this scholarly work, feel free to copy and paste the following:

Misoon Oh and Seok Kim (2012). Electrochemical Properties of Carbon-Supported Metal Nanoparticles Prepared by Electroplating Methods, Electroplating, Prof. Darwin Sebayang (Ed.), ISBN: 978-953-51-0471-1, InTech, Available from: http://www.intechopen.com/books/electroplating/electrochemical-properties-of-carbon-supported-metal-nanoparticles-prepared-by-electroplating-method

INTECH
open science | open minds

InTech Europe
University Campus STeP Ri
Slavka Krautzeka 83/A
51000 Rijeka, Croatia
Phone: +385 (51) 770 447
Fax: +385 (51) 686 166

InTech China
Unit 405, Office Block, Hotel Equatorial Shanghai
No.65, Yan An Road (West), Shanghai, 200040, China
中国上海市延安西路65号上海国际贵都大饭店办公楼405单元
Phone: +86-21-62489820
Fax: +86-21-62489821

INTECH